GEOSCIENCE FRONTIERS 3(6) (2012) 893–900

available at www.sciencedirect.com

China University of Geosciences (Beijing)

GEOSCIENCE FRONTIERS

journal homepage: www.elsevier.com/locate/gsf

RESEARCH PAPER

Effect of fracture-skin on virus transport in fractured porous media

N. Natarajan [a,*], **G. Suresh Kumar** [b]

[a] *EWRE Division, Department of Civil Engineering, Indian Institute of Technology, Madras, Chennai 36, India*
[b] *Department of Ocean Engineering, Indian Institute of Technology, Madras, Chennai 36, India*

Received 2 January 2012; received in revised form 16 March 2012; accepted 19 March 2012
Available online 3 April 2012

KEYWORDS
Fracture-skin;
Virus transport;
Rock-matrix;
Fracture

Abstract A numerical model is developed for describing the transport of virus in a fracture-matrix coupled system with fracture-skin. An advective dispersive virus transport equation, including first-order sorption and inactivation constant is used for simulating the movement of viruses. Implicit finite-difference numerical technique is used to solve the coupled non-linear governing equations for the triple continuum model consisting of fracture, fracture-skin and the rock-matrix. A varying grid is adopted at the fracture and fracture-skin interface to capture the mass transfer. Sensitivity analysis was performed to investigate the effect of various properties of the fracture-skin as well as viruses on the virus concentration in the fractured formation with fracture-skin. Simulation results suggest that the virus concentration in the fracture decreases with increment in the fracture-skin porosity, fracture-skin diffusion coefficient, mass transfer coefficient, inactivation constant and sorption distribution coefficient, and with reduction in the fracture aperture.

1. Introduction

Understanding the movement of bacteria, viruses and abiotic colloids in the subsurface formation has become an important area of research. Most of the viruses in groundwater originate from human sewage from nearby municipal wastewater discharges, septic tanks, and sanitary landfills (Keswick and Gerba, 1980). There is a possibility of groundwater contamination by biocolloids (i.e., bacteria, viruses) during reclaimed-water irrigation and direct injection of recycled water (Masciopinto et al., 2008; Chrysikopoulos et al., 2010). The occurrence of fractures in a groundwater aquifer system is a common phenomenon. As far as fractured porous media is concerned, it is a well known that the fractures play a primary role for the transport of contaminants and colloids as they are preferential pathways along which dissolved

* Corresponding author.
E-mail address: itsrajan2002@yahoo.co.in (N. Natarajan).

Peer-review under responsibility of China University of Geosciences (Beijing).
doi:10.1016/j.gsf.2012.03.004

Production and hosting by Elsevier

reactive and non-reactive contaminants and viruses can move rapidly. Pathogenic bacteria and viruses are observed to travel longer distances in fractured rock formation than in porous formation (Bales et al., 1989).

Several mathematical models have been developed for the transport of viruses in porous formations. Sim and Chrysikopoulos (1995) developed analytical solution for virus transport in one-dimensional homogeneous, saturated porous media for both constant flux as well as constant concentration boundary condition. The effect of model parameters on virus transport was investigated. Chrysikopoulos and Sim (1996) developed a stochastic model for one-dimensional virus transport in homogeneous, saturated, semi-infinite porous media. The model accounted for first-order inactivation of liquid phase and adsorbed viruses with different inactivation rate constants, and time independent distribution coefficient. Bales et al. (1997) conducted field experiments invoking virus and microsphere transport in a sandy aquifer in Borden, and experimental data were simulated by using a one-dimensional transport model with a first-order kinetic and an equilibrium mass transfer. Rehmann et al. (1999) used the stochastic approach to study the effect of spatial variability of hydraulic conductivity and virus transport parameters on virus transport through heterogeneous porous media. Sim and Chrysikopoulos (2000) developed a numerical model for one-dimensional virus transport in homogeneous, unsaturated porous media. Their model accounted for virus sorption onto liquid–solid and air–liquid interfaces as well as inactivation of viruses suspended in liquid phase and virus attached at both interfaces. Jin and Flury (2002) reviewed the current research work done on fate and transport of viruses in porous media to provide a thorough understanding of the key processes governing virus survival and transport in the natural environment. Bhattacharjee et al. (2002) developed a two-dimensional model for virus transport in physically and geochemically heterogeneous porous media. They considered both layered and randomly distributed physical and geochemical heterogeneity for the modeling of virus transport through porous media. Anders and Chrysikopoulos (2005) conducted field-scale experiment to investigate the fate and transport of viruses during artificial recharge. They also developed a numerical model to simulate virus transport in one-dimensional, homogeneous saturated porous media accounting for virus sorption, inactivation and time dependent source concentration. Masciopinto et al. (2008) investigated the fate and transport of pathogens introduced by artificial groundwater recharge in a fractured aquifer. Anders and Chrysikopoulos (2009) conducted experiment to investigate the factors that control virus inactivation as well as transport in saturated and unsaturated porous media. Chrysikopoulos et al. (2010) investigated the removal of biocolloids (bacteria and viruses) in pilot-scale fractured aquifers consisting of horizontal limestone slabs. Sharma and Srivastava (2011) developed a numerical model to simulate virus transport through two-dimensional heterogeneous porous media at field scale to investigate the effect of inactivation and mass transfer rate constants on the relative concentration profile in two observation wells. Ojha et al. (2011) recently developed a numerical model to investigate the transport processes of the movement of viruses in a fractured rock. They also simulated the experimental data of biocolloids through the fractured aquifer model.

From literature, it can be seen that numerous studies have been conducted on virus transport in porous media but only a few on virus transport through fractured porous media. However, recent investigations have suggested the role of fracture-skin at fracture-matrix interface, whose rock properties are generally found to be significantly different from that of its associated rock-matrix (Robinson et al., 1998). Sharp et al. (1993) pointed out the possibility of the presence of fracture-skins in a fractured porous media. These are defined as low-permeability material deposited along the fracture walls. A few studies conducted with respect to solute transport in fracture-skins have concluded that fracture-skins in the form of clay filling (Driese et al., 2001), mineral precipitation (Fu et al., 1994) and organic growth material (Robinson and Sharp, 1997) have reduced the permeability in fracture-skin while some others have concluded that the presence of fracture-skins has increased the permeability in fracture-skins by developing micro-fractures (Polak et al., 2003). The parameters of fracture-skin such as diffusion coefficient and porosity may significantly differ from that of the rock-matrix. It should be noted that the mass transfer mechanisms are different at the fracture-skin interface as well as the skin-matrix interface. Thus the presence of fracture-skin may either enhance or mitigate the mass transfer at the interface, and in turn influence the colloidal transport in the fractures.

Nair and Thampi (2010) developed a numerical model to describe the transport of colloids in sets of parallel fractures with fracture-skin. As far as the author's knowledge is concerned, no studies have been conducted to analyze the effect of fracture-skin on virus transport in fractured porous media. The objective of this work is to analyze the effect of various parameters of fracture-skin and viruses on the relative concentration of viruses in the fracture-matrix coupled system. Although Robinson et al. (1998) and Nair and Thampi (2010) have developed mathematical models for transport of contaminants and colloids in fractured porous media, virus transport mechanism is unique when compared to contaminants and other colloids. The purpose of this paper is to specifically analyze the evolution of virus concentration in the presence of fracture-skin in the fractured porous media. Sensitivity analysis has been performed to investigate the effect of fracture-skin parameters and virus properties on the virus concentration in the fracture.

2. Physical system and governing equations

The conceptual model corresponding to a coupled fracture-skin-matrix system (Robinson et al., 1998) is illustrated in Fig. 1.

In Fig. 1, b represents the half fracture aperture, $b - d$ represents the thickness of the fracture-skin and H represents the thickness of the half fracture spacing. The principal transport mechanisms in the fracture are advection, hydrodynamic dispersion, and solute mass transfer into the fracture-skin and rock-matrix through matrix diffusion. The transport processes in the coupled fracture-skin-matrix system can be described by three coupled equations pertaining to fracture, fracture-skin and the rock-matrix. The matrix diffusion is considered to be one-dimensional, taking place in the direction perpendicular to the fracture. This can be justified because solute migration is faster in the fracture than in the matrix based on the studies conducted by Kennedy and Lennox (1995) who showed numerically that such assumptions are valid for most cases, except for fractured clay with fracture apertures less than 20 μm and flow velocity lower than 1 m/d. A constant groundwater velocity is assumed in the fracture. Virus transport in saturated porous media with first-order sorption and inactivation is governed by the following equation (Sim and Chrysikopoulos, 1995).

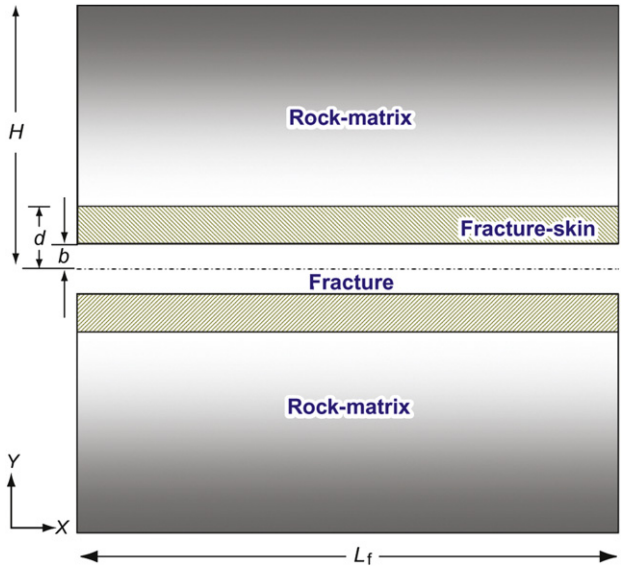

Figure 1 Schematic diagram showing a coupled fracture-skin-matrix system.

$$\frac{\partial C_s}{\partial t}+\frac{\rho_s}{\theta_s}\frac{\partial S_s}{\partial t}=D_L\frac{\partial^2 C_s}{\partial x^2}+D_s\frac{\partial^2 C_s}{\partial y^2}-V\frac{\partial C_s}{\partial x}-\lambda_c C_s-\lambda_s\frac{\rho_s}{\theta_s}S_s \tag{1}$$

where C_s = concentration of virus in suspension in the fracture-skin (M/L^3), S_s = mass of virus adsorbed on the porous fracture-skin (M/M), D_L = longitudinal hydrodynamic dispersion coefficient (L^2/T), D_s = effective diffusion coefficient of fracture-skin (L^2/T), V = average pore water velocity (L/T), ρ_s = bulk density of the fracture-skin (M/L^3), λ_c = inactivation constant of suspended viruses (T^{-1}), λ_s = inactivation constant of sorbed viruses (T^{-1}), θ_s = fracture-skin porosity, t = time (T).

$$\frac{\partial C_m}{\partial t}+\frac{\rho}{\theta_m}\frac{\partial S_m}{\partial t}=D_L\frac{\partial^2 C_m}{\partial x^2}+D_m\frac{\partial^2 C_m}{\partial y^2}-V\frac{\partial C_m}{\partial x}-\lambda_c C_m-\lambda_s\frac{\rho}{\theta_m}S_m \tag{2}$$

where C_m = concentration of virus in suspension in the rock-matrix (M/L^3), S_m = mass of virus adsorbed on the porous rock-matrix (M/M), D_L = longitudinal hydrodynamic dispersion coefficient (L^2/T), D_m = effective diffusion coefficient of fracture-skin (L^2/T), V = average pore water velocity (L/T), ρ_m = bulk density of the fracture-skin (M/L^3), λ_c = inactivation constant of suspended viruses (T^{-1}), λ_s = inactivation constant of sorbed viruses (T^{-1}), θ_m = rock-matrix porosity, t = time (T).

With the assumption that the adsorption process consists of virus diffusion to the outer layer of a solid particle by non-equilibrium mass transfer and virus immobilization onto the solid particle, while in equilibrium with liquid-phase virus concentration in the outer layer, the sorption term in Eqs. (1) and (2) can be written as (Sim and Chrysikopoulos, 1996).

$$\frac{\rho}{\theta}\frac{\partial S}{\partial t}=k(C-C_g)-\lambda_s\frac{\rho}{\theta}S \tag{3}$$

where k = mass transfer rate constant (T^{-1}), C_g = liquid-phase virus concentration in direct contact with solids (M/L^3).

Experiments showed that for low liquid phase virus concentration and when virus affinity for the adsorbent is small, the non-linear form of the Langmuir isotherm can be used (Sim and Chrysikopoulos, 1995).

$$C_g=\frac{S}{K_d} \tag{4}$$

where K_d = partition distribution coefficient (L^3/M).

The transport equation including linear equilibrium sorption and first-order degradation coefficient for the fracture can be written as (Tang et al., 1981):

$$\frac{\partial C_f}{\partial t}=-\frac{V_f}{R_f}\frac{\partial C_f}{\partial x}+\frac{D_f}{R_f}\frac{\partial^2 C_f}{\partial x^2}-\lambda_c C_f+\left.\frac{\theta_s D_s}{bR_f}\frac{\partial C_s}{\partial y}\right|_{y=b} \tag{5}$$

where $D_f=\alpha_f V_f+D_o$, V_f = velocity of water in the fracture (L/T), b = half-fracture aperture (L), D_f = hydrodynamic dispersion coefficient (L^2/T), D_o = molecular diffusion coefficient of the solute in free water (L^2/T), D_s = effective diffusion coefficient in the fracture-skin (L^2/T), α_f = longitudinal dispersivity in the fracture (L), R_f = retardation factor for fracture, λ_c = first-order degradation coefficient of solute (T^{-1}), x and y = spatial coordinates along the fracture and rock-matrix, t = time (T).

The following initial and boundary conditions have been used in developing the numerical model.

$$C_f(x,\,t=0)=0,\quad C_f(x=0,\,t)=C_0,\quad \frac{\partial C_f}{\partial x}(x=L_f,\,t)=0 \tag{6}$$

$$S_m(x,\,y,\,t=0)=0,\quad S_s(x,\,y,\,t=0)=0 \tag{7}$$

$$C_m(x,\,y,\,t=0)=0,\quad C_s(x,\,y,\,t=0)=0 \tag{8}$$

$$C_f(x,\,t)=C_s(x,\,y=b,\,t) \tag{9}$$

$$\theta_s D_s\frac{\partial C_s(x,\,y=d,\,t)}{\partial y}=\theta_m D_m\frac{\partial C_m(x,\,y=d,\,t)}{\partial y} \tag{10}$$

$$C_s(x,\,y=d,\,t)=C_m(x,\,y=d,\,t) \tag{11}$$

$$\frac{\partial C_m(x,\,y=H,\,t)}{\partial y}=0 \tag{12}$$

where C_0 is the virus concentration at the inlet of the fracture (M/L^3).

3. Numerical solution

In this study, the system is described by a set of three partial differential equations for virus; one for the fracture, another for the fracture-skin, and another for the rock-matrix formulated for a one-dimensional framework. The continuity at the fracture-matrix interface is attained by iterating the solution at each time step. The coupled system is solved numerically using implicit finite difference scheme. The advection part is discretized using upwind scheme and the diffusion part using second order central difference scheme. A varying cell width is adopted in the porous skin to capture the flux transfer at the fracture-skin interface.

Within every time step, first fracture equation is solved, and then the concentration of the fracture is used to solve the governing equations for the fracture-skin. Further, the solution from the fracture-skin is used to solve the rock-matrix equations. The discretization of the coupling term representing the last term on the right hand side of Eq. (5), involves the difference in the fracture/skin concentrations over the fracture-skin interface between the second and first nodes of fracture-skin. Thus the coupling term in Eq. (5) is discretized as

$$\frac{\partial C_s}{\partial y} = \frac{C_{s\,2}^{n+1} - C_{s\,1}^{n+1}}{\Delta y_s(1)} \quad (13)$$

where Δy_s (1) represents the cell width across the fracture-skin interface.

Here the concentration at the first node in the fracture-skin, i.e., $C_{s\,1}^{n+1}$, will be equal to the corresponding fracture concentration $(C_{f\,i}^{n+1}|_{i=1})$ perpendicular to the fracture-skin satisfying assumed boundary condition, that is,

$$C_{s\,1}^{n+1} = C_{f\,1}^{n+1} \quad (14)$$

The concentration of the second node in the fracture-skin, $C_{s\,2}^{n+1}$, at unknown at the next time level, $(n + 1)^{th}$ time level, it will become fourth unknown. The value of this unknown is assumed and iterated till convergence. Thus using Tridiagonal Thomas Algorithm (TTA), the three unknowns that are solved for the fracture are at I^{th} node, $(I - 1)^{th}$ node and $(I + 1)^{th}$ node, at $(n + 1)^{th}$ time level. Thus, the fourth unknown, the concentration at the second node of the skin at $(n + 1)^{th}$ level, $C_{s\,2}^{n+1}$ is not solved by TTA solver as its value is assumed at $(n + 1)^{th}$ level and iterated until convergence.

4. Results and discussion

The influence of fracture-skin on the transport of viruses is analyzed in a fracture-matrix coupled system in the presence of fracture-skin. Since analytical solutions are not available for virus transport in fractured media in the presence of fracture-skin, the numerical model has been validated with the analytical solution provided by Robinson et al. (1998) and Tang et al. (1981) for cases with and without skin. The dataset used for the validation of the numerical model with Robinson et al. (1998) and Tang et al. (1981) has been provided in Tables 1 and 2. The parameters used for development of the numerical model for simulation of viruses in coupled fracture-skin-matrix system are presented in Table 3.

Fig. 2a and b represents the comparison of the results obtained from the present numerical model with the analytical solution provided by Robinson et al. (1998) and Tang et al. (1981). It is observed from Fig. 2a and b that the present model is in close agreement with the analytical solution for the cases with and without fracture-skin.

Fig. 3 illustrates the comparison of the virus concentration in the fracture in the presence and absence of fracture-skin. It is observed from Fig. 3 that the spatial distribution of virus concentration at the inlet of the fracture varies for both the cases. In the absence of fracture-skin, the virus concentration profile gradually reduces from the source and reaches zero concentration at 105 m from the inlet of the fracture. On the other hand, due to the presence of fracture-skin, the virus concentration remains constant for a significant section of the fracture and reduces drastically to zero at 125 m from the fracture inlet. Thus, the presence of fracture-skin causes a drastic variation in the virus concentration along the fracture as observed from the figure. Therefore, fracture-skin is an important aspect that needs to be considered while investigating the movement of viruses in fractured porous media.

Fig. 4 illustrates the spatial distribution of virus concentration along the fracture for various fracture-skin porosities. It is observed from Fig. 4 that high fracture-skin porosities enhance the diffusion of viruses into the fracture-skin resulting in very low virus concentration along the fracture. High fracture-skin porosity

Table 1 Dataset used for validation of numerical model with fracture-skin.

Parameter	Value
Average fluid flow velocity in fracture (V_o)	1.0 m/d
Fracture dispersivity (α_o)	0.001 m
Longitudinal dispersion coefficient within the fracture (D_L)	1×10^{-3} m^2/d
Free molecular diffusion coefficient in water ($D^{*)}$	1×10^{-6} m^2/d
Effective diffusion coefficient in the rock-matrix (D_m)	4×10^{-6} m^2/d
Effective diffusion coefficient in the fracture-skin (D_s)	4×10^{-7} m^2/d
Porosity of rock-matrix (θ_m)	0.145
Porosity of fracture-skin (θ_s)	0.0145
Length of fracture (L_f)	100 m
Fracture spacing ($2H$)	0.31 m
Half fracture aperture (b)	0.0002 m
Fracture-skin thickness ($d - b$)	0.0018 m
Total simulation time (tst)	10 d

Table 2 Parameters used for validation of the numerical model without fracture-skin.

Parameter	Value
Initial fracture aperture ($2b$)	10,000 μm
Fluid velocity (V)	1 m/d
Porosity of the rock-matrix (θ_m)	0.01
Longitudinal fracture dispersivity (α_L)	0.5 m
Free molecular diffusion coefficient (D^*)	1×10^{-5} m^2/d
Matrix diffusion coefficient (D_m)	1×10^{-5} m^2/d
Length of the fracture (L_f)	50 m
Total simulation time (T)	25 d

Table 3 Parameters used for the simulation of virus transport in fracture-skin-matrix system.

Parameter	Value
Fracture velocity (V_f)	1 m/d
Local dispersivity (α_f)	0.5 m
Fracture aperture (b)	50 μm
Inactivation constant in fracture (λ_c)	0.001 d^{-1}
Fracture spacing (L)	0.01 m
Matrix porosity (θ)	0.02 m
Fracture retardation factor (R_f)	1
Bulk density of soil (ρ)	1.5 g/mL
Longitudinal dispersivity (α_L)	0.5 m
Effective diffusion (D_m)	1×10^{-10} m^2/d
Pore water velocity (V)	0.5 m/d
Distribution coefficient (K_d)	0.2 mL/g
Mass transfer constant (k)	0.01 h^{-1}
Inactivation constant in fracture-skin and rock-matrix	0.006 d^{-1}
Total simulation time (T)	100 d

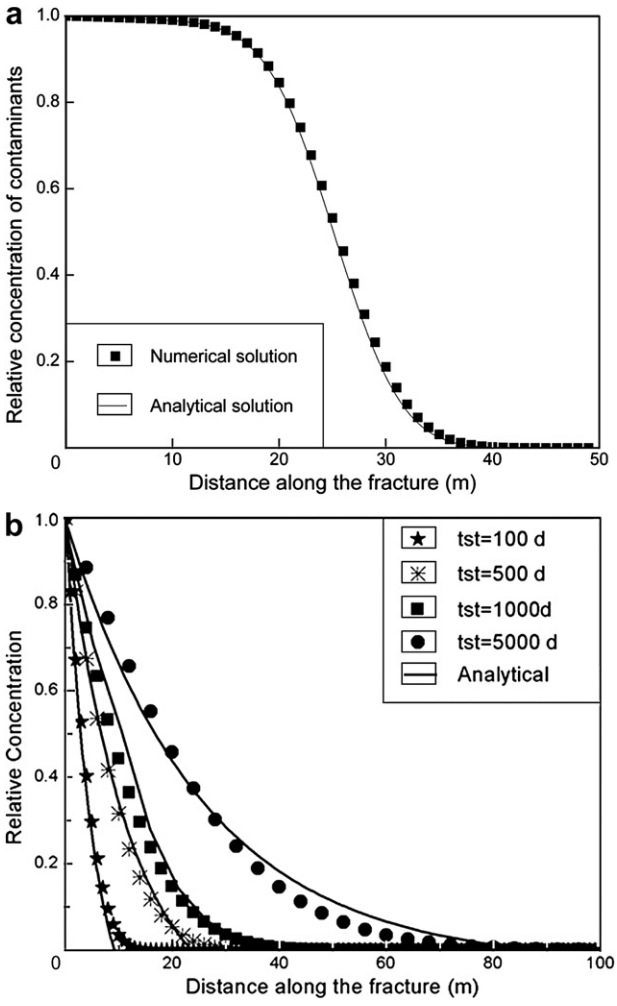

Figure 2 Comparison of the results obtained from the present numerical model with analytical solution of Tang et al. (1981) (a) and Robinson et al. (1998) (b). $R_f = 6$, $R_s = 673$, $R_m = 141$, $\lambda = 6.33 \times 10^{-5}$ d^{-1}.

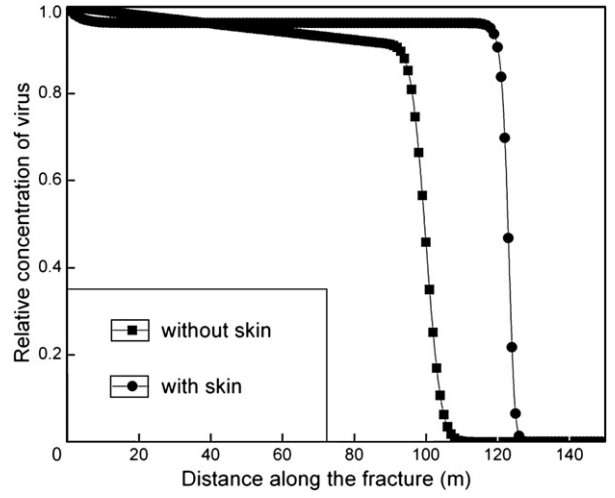

Figure 3 Spatial distribution of virus concentration in the fracture in the presence and absence of fracture-skin. Refer Table 3 for data.

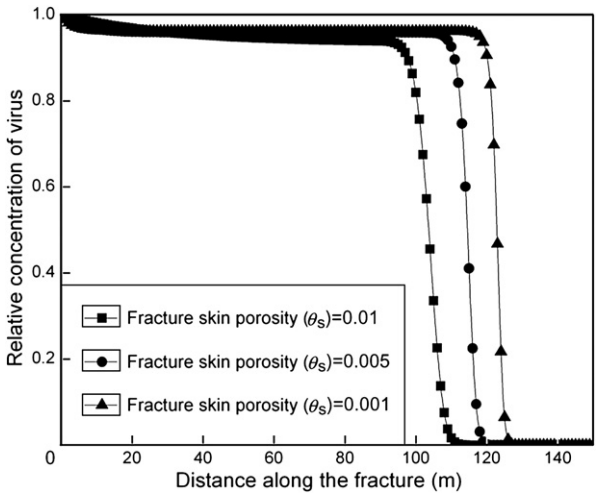

Figure 4 Spatial distribution of virus concentration along the fracture for various fracture-skin porosities. Refer Table 3 for data.

provides a medium for significant sorption of virus on the fracture wall surface. As the fracture-skin porosity is decreased, the diffusion of viruses is significantly decreased and thus the virus concentration gradually increases along the fracture. The virus concentration becomes zero farther away from the fracture inlet with decrement in fracture porosity.

Fig. 5 illustrates the spatial distribution of virus concentration along the fracture for various fracture-skin diffusion coefficients. It is observed from Fig. 5 that high fracture-skin diffusion co-efficient ($D_s = 1 \times 10^{-7}$ m^2/d) increases the diffusion of viruses into the fracture-skin resulting in very low virus concentration along the fracture. Further reduction of the skin diffusion co-efficient to 1×10^{-9} m^2/d does not affect the virus concentration profile significantly but when the skin diffusion coefficient is very low ($D_s = 1 \times 10^{-11}$ m^2/d), the diffusion of viruses into the fracture-skin is very low and consequently the concentration of viruses in the fracture reaches zero after 120 m from the fracture inlet. Even at the inlet of the fracture, it is observed that the virus concentration

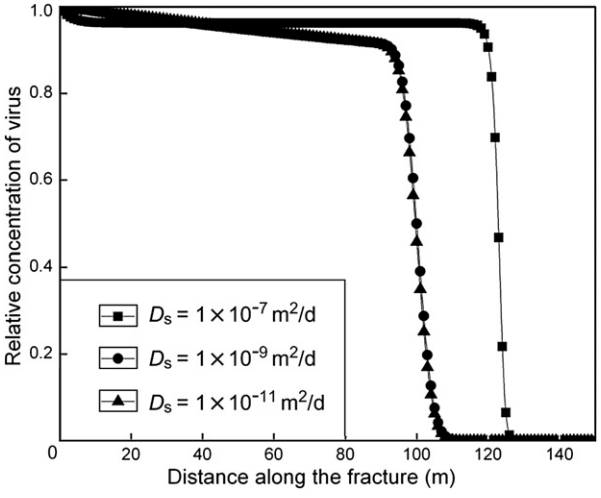

Figure 5 Spatial distribution of virus concentration along the fracture for various fracture-skin diffusion coefficients. Refer Table 3 for data.

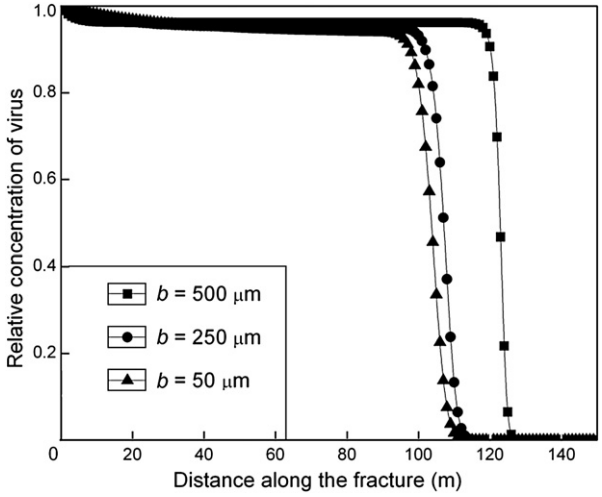

Figure 6 Spatial distribution of virus concentration along the fracture for different half fracture apertures. Refer Table 3 for data.

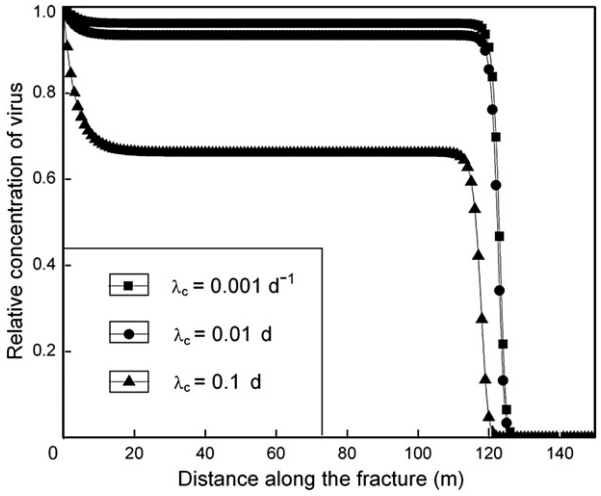

Figure 8 Spatial distribution of virus concentration along the fracture for different inactivation constants. Refer Table 3 for data.

profile for very low diffusion coefficient is marginally different from other cases.

Fig. 6 illustrates the spatial distribution of virus concentration along the fracture for different half fracture apertures. It is observed from Fig. 6 that as the fracture aperture increases, the concentration of viruses in the fracture decreases. This is because the small fracture aperture results in a strong coupling between the fracture and the adjacent fracture-skin which enhances the diffusion of viruses into the fracture-skin resulting in very low virus concentration along the fracture. With increment in the fracture aperture, the coupling weakens and the concentration of the virus along the fracture increases.

Fig. 7 illustrates the spatial distribution of virus concentration along the fracture for different mass transfer coefficient. It is observed from Fig. 7 that as the mass transfer coefficient is increased, the concentration of virus decreases along the fracture. This observation is similar to that observed by Ojha et al. (2011) but the pattern of the concentration profile is completely different due to the presence of fracture-skin. When the mass transfer coefficient is zero, the relative concentration of viruses in the fracture remains as 1 up to 125 m of the fracture length. With increment of the mass transfer coefficient to 0.01 d^{-1}, the relative concentration starts reducing very close to the fracture inlet and remains constant thereafter for a larger portion of the fracture. When the mass transfer coefficient is assumed to be 0.1 d^{-1}, the concentration of the virus significantly reduces at the inlet of the fracture due to the presence of fracture-skin and remains constant for some distance before becoming zero. As observed from the above plot, virus transport mechanism is affected by the presence of fracture-skin due to its influence on the mass transfer at the interface of the fracture and the rock-matrix.

Fig. 8 illustrates the spatial distribution of virus concentration along the fracture for different inactivation constants. It is observed from Fig. 8 that as the inactivation constant increases, the concentration of viruses decreases along the fracture. When the mass transfer coefficient is very low, the relative concentration of viruses is observed over a larger length of the fracture. There is a marginal variation with the increment of the inactivation constant to 0.01 d^{-1}. When the mass transfer coefficient is

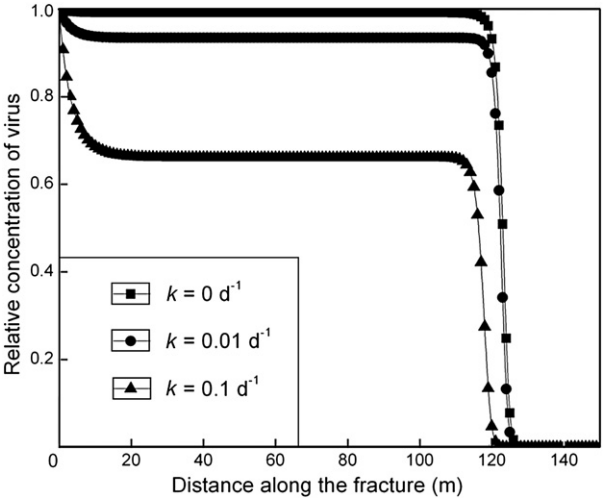

Figure 7 Spatial distribution of virus concentration along the fracture for different mass transfer coefficients. Refer Table 3 for data.

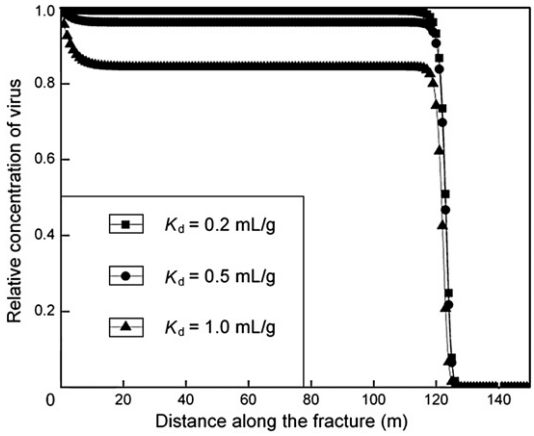

Figure 9 Spatial distribution of virus concentration along the fracture for different sorption distribution coefficients. Refer Table 3 for data.

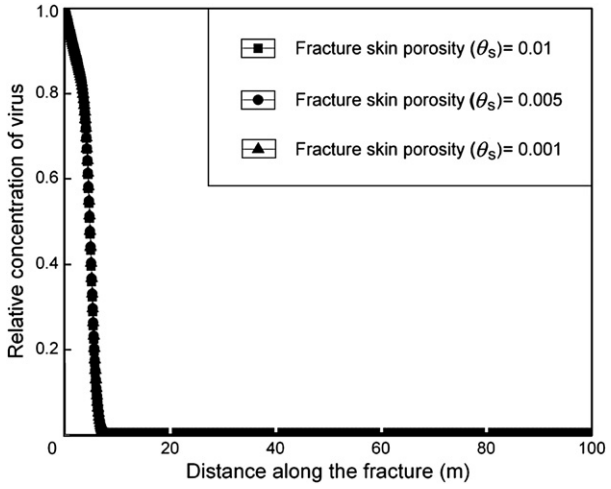

Figure 10 Spatial distribution of virus concentration along the fracture for different fracture-skin porosities using field data from Chrysikopoulos et al. (2010) (fracture flow velocity = 42 m/d, length of the fracture = 150 m, fracture aperture = 0.00005 m, fracture spacing = 0.01 m, fracture dispersivity = 0.2 m, diffusion coefficient = 1×10^{-11} m^2/d).

increased to 0.1 d^{-1}, the concentration of the virus significantly reduces at the inlet of the fracture due to the presence of fracture-skin and remains constant before becoming zero. Unlike the fracture-matrix coupled system, where there is an exponential reduction in the concentration of virus for large inactivation constants, the concentration profile follows a different pattern due to the presence of the fracture-skin.

Fig. 9 illustrates the spatial distribution of virus concentration along the fracture for different sorption distribution coefficients. It is observed from Fig. 9 that the variation of the sorption distribution coefficient has very marginal effect on the virus concentration along the fracture. For very large sorption coefficients, the concentration of the virus significantly reduces at the inlet of the fracture and then remains constant before merging with other concentration profiles. Thus, the presence of fracture-skin has very less impact on the sorption coefficient of viruses in the fracture-matrix coupled system.

Fig. 10 illustrates the application of the model using field data provided by Chrysikopoulos et al. (2010). It is observed from Fig. 10 that the virus concentration profiles are same for all fracture-skin porosities. This is because of the high fluid velocity of 42 m/d along the fracture which minimizes the interaction between the fracture-skin and the fracture. Consequently, the residence time available for diffusion of viruses into the fracture-skin is significantly reduced.

5. Conclusions

A numerical model is developed to analyze the transport of viruses in a coupled fracture-matrix system in the presence of fracture-skin. The set of coupled equations for virus transport in the fracture-skin-matrix system is solved using implicit finite difference method. Constant continuous source of virus is assumed at the inlet of the fracture. The flux transfer at the interface of the fracture and the fracture-skin is captured by adopting a varying grid pattern. The presence of fracture-skin significantly affects the virus transport mechanism in the coupled fracture-matrix system.

Virus concentration along the fracture decreases along the fracture with increment in fracture porosity as the high fracture-skin porosity provides a medium for significant sorption of virus on the fracture wall surface. High fracture-skin diffusion co-efficient increases the diffusion of viruses into the fracture-skin resulting in very low virus concentration along the fracture and there is no variation in the virus concentration with reduction of skin diffusion coefficient below 1×10^{-9} m^2/d. The small fracture apertures provide a strong coupling between the fracture and the adjacent fracture-skin thereby causing a reduction in the virus concentration along the fracture. The presence of fracture-skin affects the mass transfer mechanism at the interface of the fracture and the rock-matrix. Consequently, the virus concentration profiles vary in their behavior along the fracture for various mass transfer coefficients. The presence of fracture-skin produces an exponential reduction in the concentration of virus for large inactivation constants unlike the fracture-matrix coupled system. The variation of the sorption distribution coefficient has very marginal effect on the virus concentration along the fracture in the presence of fracture-skin. Thus, the presence of fracture-skin has very less impact on the sorption coefficient of viruses in the fracture-matrix coupled system. For high inactivation constants, partition coefficients as well as mass transfer coefficients, the virus concentration significantly reduces at the inlet of the fracture due to the presence of fracture-skin.

References

Anders, R., Chrysikopoulos, C.V., 2005. Virus fate and transport during artificial recharge with recycled water. Water Resources Research 41, W10415.

Anders, R., Chrysikopoulos, C.V., 2009. Transport of viruses through saturated and unsaturated columns packed with sand. Transport in Porous Media 76, 121–138.

Bales, R.C., Gerba, C.P., Grondin, G.H., Jensen, S.L., 1989. Bacteriophage transport in sandy soil and fractured tuff. Applied and Environment Microbiology 55, 2061–2067.

Bales, R.C., Li, S., Yeh, T.C.J., Lenczewski, M.E., Gerba, C.P., 1997. Bacteriophage and microsphere transport in saturated porous media: forced-gradient experiment at Borden, Ontario. Water Resources Research 33 (4), 639–648.

Bhattacharjee, S., Ryan, J.N., Elimelech, M., 2002. Virus transport in physically and geochemically heterogeneous subsurface porous media. Journal of Contaminant Hydrology 57, 161–187.

Chrysikopoulos, C.V., Masciopinto, C., La Mantia, R., Manariotis, I.D., 2010. Removal of biocolloids suspended in reclaimed wastewater by injection in a fractured aquifer model. Environmental Science and Technology 44 (3), 971–977.

Chrysikopoulos, C.V., Sim, Y., 1996. One dimensional virus transport in homogeneous porous media with time-dependent distribution coefficient. Journal of Hydrology 185, 199–219.

Driese, S.G., McKay, L.D., Penfield, C.P., 2001. Lithologic and pedogenic influences on porosity distribution and groundwater flow in fractured sedimentary saprolite: a new application of environmental sedimentology. Journal of Sedimentology Research 71 (5), 843–857.

Fu, K.L., Milliken, J.M., Sharp Jr., J.M., 1994. Porosity and permeability variations in fractured and liesegang-banded Breathirr sandstones (middle Pennsylvanian), eastern Kentucky: diagenetic controls and implications for modeling dual-porosity systems. Journal of Hydrology 154, 351–381.

Jin, Y., Flury, M., 2002. Fate and transport of viruses in porous media. Advances in Agronomy 77, 40–102.

Kennedy, C.A., Lennox, W.C., 1995. A control volume model of solute transport in a single fracture. Water Resources Research 31 (2), 313–322.

Keswick, B.H., Gerba, C.P., 1980. Viruses in groundwater. Environmental Science and Technology 14, 1290−1297.

Masciopinto, C., La Mantia, R., Chrysikopoulos, C.V., 2008. Fate and transport of pathogens in a fractured aquifer in the Salento area, Italy. Water Resources Research 44, W01404.

Nair, V.V., Thampi, S.G., 2010. Numerical modeling of colloid transport in sets of parallel fractures with fracture skin. Colloids and Surfaces A: Physicochemical and Engineering Aspects 364, 109−115.

Ojha, C.S.P., Surampalli, R.Y., Sharma, P.K., Joshi, N., 2011. Breakthrough curves and simulation of virus transport through fractured porous media. Journal of Environmental Engineering 137 (8), 731−739.

Polak, A., Grader, A.S., Wallach, R., Nativ, R., 2003. Chemical diffusion between a fracture and the surrounding matrix, measurement by computed tomography and modeling. Water Resources Research 39 (4), 1106.

Rehmann, L.L.C., Welty, C., Harvey, R.W., 1999. Stochastic analysis of virus transport in aquifers. Water Resources Research 35 (7), 1987−2006.

Robinson, N.I., Sharp, J.M., Kreisel, I., 1998. Contaminant transport in sets of parallel finite fractures with fracture skins. Journal of Contaminant Hydrology 31, 83−109.

Robinson, N.I., Sharp Jr., J.M., 1997. Analytical Solution for Contaminant Transport in a Finite Set of Parallel Fractures with Matrix Diffusion, C.S.I.R.O. Mathematical and Information Sciences Report CMIS-C23, pp. 26.

Sim, Y., Chrysikopoulos, C.V., 1995. Analytical models for one-dimensional virus transport in saturated porous media. Water Resources Research 31 (5), 1429−1437.

Sim, Y., Chrysikopoulos, C.V., 2000. Virus transport in unsaturated porous media. Water Resources Research 36 (1), 173−179.

Sharma, P.K., Srivastava, R., 2011. Numerical analysis of virus transport through heterogeneous porous media. Journal of Hydro-environmental Research 5, 93−99.

Sharp, J.M., Smyth-Boulton, R.C., Fuller, C.M., 1993. Permeability-porosity variations and fracture patterns in tuffs. In: Banks, D., Banks, S. (Eds.), Hydrogeology of Hard Rocks, Memoires of the 24th Cong. International Assoc. Hydrogeologists, Oslo, Norway, 24, part 1, pp. 103−114.

Sim, Y., Chrysikopoulos, C.V., 1996. Correction to: analytical models for one-dimensional virus transport in saturated porous media. Water Resources Research 32 (5), 1473.

Tang, D.H., Frind, E.O., Sudicky, E.A., 1981. Contaminant transport in fractured porous media: analytical solution for a single fracture. Water Resources Research 17 (3), 555−564.